

# Deep Quaternion Neural Network for 3D Sound Source Localization and Detection

Project of Neural Network Course, Prof. Uncini

Sveva Pepe 1743997  
Marco Pennese 1749223  
Claudia Medaglia 1758095

## 1 Introduction

Sound source localization is a fundamental task, especially in reverberant and multiple sources environments; it includes recognizing the temporal onset and offset of sound events when active, classifying the sound events into known set of classes, and further localizing the events in space when active using their direction of arrival (DOA).

In this project, we work with 3D audio sounds captured by first-order Ambisonic microphone and these sounds are then represented by spherical harmonics decomposition in the quaternion domain.

The aim of the project is to detect the temporal activities of a known set of sound event classes and to further locate them in the space using quaternion-valued data processing, in particular we focus on the sound event localization and detection (SELD).

In order to do this, we use a given Quaternion Convolutional Neural Network with the addition of some recurrent layers (QCRNN) for the joint 3D sound event localization and detection task.

## 2 Quaternion domain

3D audio files are sampled using the Ambisonics technique, where sampling is based on the decomposition of sound in a linear combination of orthogonal bases of spherical harmonics.

In this project the first-order Ambisonics (FOA) was considered, which is composed of 4 microphone capsules. The first is a pressure microphone, the other three are orthogonal eight-shaped microphones related to the pressure gradient, or the acoustic speed.

The pressure microphone is an omnidirectional microphone that has unity gain in all directions. It is indicated by the letter W and corresponds to the spherical harmonic function of order 0. Instead the other three microphones are denoted respectively with X, Y, Z and correspond to the harmonic functions of order 1.

Our goal is to use spherical harmonics in the quaternion domain, so let's consider four ambisonic signals, namely  $x_W[n]$ ,  $x_X[n]$ ,  $x_Y[n]$  e  $x_Z[n]$ , as a single quaternion signal:

$$x[n] = x_W[n] + x_X[n]\hat{i} + x_Y[n]\hat{j} + x_Z[n]\hat{k}$$

where  $x[n]$  is quaternion-valued ambisonic signal and the four components define the B-Ambisonics format, in fact, we have:

$$\begin{cases} x_W[n] = \frac{s[n]}{\sqrt{3}} \\ x_X[n] = s[n] \cos(\theta) \cos(\varphi) \\ x_Y[n] = s[n] \sin(\theta) \cos(\varphi) \\ x_Z[n] = s[n] \sin(\varphi) \end{cases}$$

The factor  $\frac{1}{\sqrt{3}}$  to the omnidirectional microphone allows to attenuate the average energy of that channel by 3 dB about on the full sphere, thus making it equal to the average energy of all the other channels.

We note that  $x_W[n]$  is the real component of the quaternion signal, while the  $x_X[n]$ ,  $x_Y[n]$  and  $x_Z[n]$  are considered the imaginary components.

Now we have to derive the quaternion-value input features that will be passed to the network, to do this we need the acoustic intensity.

The vector of acoustic intensity, also called sound field, is produced by average of the sound pressure,  $p[n]$ ,

and the particle velocity,  $v[n]$ , over time:

$$I[n] = p[n] \cdot v[n]$$

In addition, the sound field provides the magnitude and direction of the flow of sound energy.

Since we are using the representation of quaternions with the B-format Ambisonic we are going to rewrite the sound pressure and speed.

Sound pressure is defined by the signal captured by the omnidirectional signal,  $p[n] = x_W[n]$ . While the particle

velocity is defined by the three orthogonal figure-of-eight microphone signals,  $v[n] = \frac{-1}{p_0 c \sqrt{3}} \cdot \begin{bmatrix} x_X[n] \\ x_Y[n] \\ x_Z[n] \end{bmatrix}$

where  $p_0$  is the mean density of the air and  $c$  is the speed of the sound.

We express the acoustic intensity in the discrete time-frequency domain in terms of pressure  $p[k, n]$  and particle with complex velocity  $v[k, n]$ , where  $k$  indicates the index of the frequency bin.

So the acoustic intensity will be equal to:

$$I[k, n] = p^*[k, n] \cdot v[k, n] = I_a[k, n] + jI_r[k, n]$$

where  $*$  denotes the complex conjugation.

$I_a$  and  $I_r$  are the two components that make up the acoustic intensity, respectively the active and reactive intensity.

Active intensity is the time average of the acoustic intensity:

$$I_a[k, n] = \Re\{p^*[k, n] \cdot v[k, n]\}$$

which corresponds to transport of sound energy and whose mean value is non-zero.

Reactive intensity is defined as the imaginary counterpart of active intensity:

$$I_r[k, n] = \Im\{p^*[k, n] \cdot v[k, n]\}$$

which corresponds to the dissipative energy transport and whose mean value is zero.

Since the intensity vectors contain the information of the acoustical energy direction of a sound wave, the acoustic intensity vector can be directly used for DOA estimation, used in localization.

In theory, the sound DOA can be estimated as the opposite direction of the active intensity vector. In practice, however, the estimates obtained across all time-frequency bins are inconsistent in reverberant environments.

Active intensity refers directly to DOA, while reactive intensity indicates whether a given frequency-time bin is dominated by sound directed by a single source, opposed to overlapping sources or reverberation.

In this way, the active and reactive intensity vectors are both extracted from the spectrogram from each audio channel and are used as separate functions.

We use both the active and reactive intensity vectors across all frequency bins in the STFT domain as input features, in particular, in order to represent the active and reactive intensity vectors we encapsulate the information in two quaternions.

Since we have three components for each intensity vector, we also consider one more channel related to the magnitude of the omnidirectional microphone signal in order to improve the performances of the localization task.

Input features can be expressed by the two quaternions  $q_a[k, n]$  and  $q_r[k, n]$ :

$$\begin{aligned} q_a[k, n] &= \Re\{x_W^*[k, n] \cdot x_W[k, n]\} \\ &\quad + \Re\{x_W^*[k, n] \cdot x_X[k, n]\}\hat{i} \\ &\quad + \Re\{x_W^*[k, n] \cdot x_Y[k, n]\}\hat{j} \\ &\quad + \Re\{x_W^*[k, n] \cdot x_Z[k, n]\}\hat{k} \\ q_r[k, n] &= \Im\{x_W^*[k, n] \cdot x_W[k, n]\} \\ &\quad + \Im\{x_W^*[k, n] \cdot x_X[k, n]\}\hat{i} \\ &\quad + \Im\{x_W^*[k, n] \cdot x_Y[k, n]\}\hat{j} \\ &\quad + \Im\{x_W^*[k, n] \cdot x_Z[k, n]\}\hat{k} \end{aligned}$$

We normalize each time-frequency bin by its total energy  $\epsilon_T = \epsilon_P + \epsilon_K$ , where  $\epsilon_P = |x_W[k, n]|^2$  is the potential energy density related to the sound pressure and  $\epsilon_K = \frac{1}{3}(|x_X[k, n]|^2 + |x_Y[k, n]|^2 + |x_Z[k, n]|^2)$  is the kinetic energy density related to the particle velocity.

Now can we express the normalize quaternion inputs as:

$$\bar{q}_a[k, n] = \frac{q_a[k, n]}{\epsilon_T}$$

$$\bar{q}_r[k, n] = \frac{q_r[k, n]}{\epsilon_T}$$

The proposed model receives the quaternion ambisonic recording, from which it extracts the spectrogram in terms of magnitude and phase components using a Hamming window of length  $M$ , an overlap of 50%, and considering only the  $\frac{M}{2}$  positive frequencies without the zeroth bin. herefore, from the two quaternion inputs, we obtain a feature sequence of  $T$  frames, with an overall dimension of  $T \times \frac{M}{2} \times 8$ .

### 3 Network Structure

The model receives as input the quaternions, from which it extracts the spectrogram in terms of magnitude and phase components using a Hamming window.

The network is a Quaternion Convolutional Recurrent Neural Network (QCRNN). In particular, we have three convolutional layers based on quaternions (QCNN), two recurrent layers (QRNN) and finally two parallel outputs, both are composed of two fully-connected layers, which obviously differ in their activation functions and size that receive input from previous layers.

The QCNN are composed of  $P$  filter kernels with size  $3 \times 3 \times 8$ .

The three convolutional networks (QCNN) consist of 3 stages: Convolutional, Detector and Pooling.

The first stage consists of the convolutional process to the inputs. Since these are quaternions, the convolutional process consists of Hamilton's product:

$$\begin{aligned} W \otimes x = & (W_w x_w - W_x x_x - W_y x_y - W_z x_z) \\ & + (W_w x_x + W_x x_w + W_y x_z - W_z x_y) \hat{i} \\ & + (W_w x_y - W_x x_z + W_y x_w + W_z x_x) \hat{j} \\ & + (W_w x_z + W_x x_y - W_y x_x - W_z x_w) \hat{k} \end{aligned}$$

where  $x$  is the vector of the quaternions taken as input and  $W$  a generic quaternion filter matrix.

Hamilton product allows quaternion neural networks to capture internal latent relations within the features of a quaternion.

After it is applied the Batch Normalization, a technique for improving the speed, performance, and stability of artificial neural networks. It is used to normalize the input layer by adjusting and scaling the activations. Also, batch normalization allows each layer of a network to learn by itself a little bit more independently of other layers.

The second phase concerns the choice of the activation function, which in the case of the three quaternion convolutional layer is the ReLU.<sup>1</sup>

For a generic quaternion dense layer we have:

$$y = \alpha(W \otimes x + b)$$

where  $y$  is the output of the layer,  $b$  is the bias offset and  $\alpha$  is quaternion activation function.

Indeed,  $\alpha(q) = f(q_w) + f(q_x) + f(q_y) + f(q_z)$ ,  $q$  is a generic quaternion and  $f$  is rectified linear unit (ReLU) activation function. As we can see, The ReLU is applied to both the real and imaginary part of the quaternion.

The last stage is the one related to Pooling. Pooling decrease the computational power required to process the data through dimensionality reduction. Furthermore, it is useful for extracting dominant features which are rotational and positional invariant, thus maintaining the process of effectively training of the model. In our network we use MaxPooling. MaxPooling is done by applying a max filter to non-overlapping subregions of the initial representation.

Max-pooling is applied along the frequency axis for dimensionality reduction while preserving the sequence length  $T$ , we obtain in the end that the output of the 3 QCNN has dimension  $T \times 8P$  and fed to bidirectional QRNN layers to better catch the time progress of the input signals.

The network also uses the Dropout technique, which consists in randomly removing network units with some probability  $\beta$ .

QRNN are recurring neural networks based on quaternions. The peculiarity of recurrent neural networks is that they differ from feedforward nets because they include a feedback loop, whereby output from step  $n-1$  is fed back to the net to affect the outcome of step  $n$ , and so forth for each subsequent step.

In these QRNN  $Q$  nodes of quaternion gated recurrent units (QGRU) are used in each layer and as a function of activation a hyperbolic tangent ( $\tanh$ ).

---

<sup>1</sup>ReLU stands for rectified linear unit, and is a type of activation function. Mathematically, it is defined as  $y = \max(0, x)$  where  $y$  is the output and  $x$  is the input.

The output of the recurrent layer is shared between two fully-connected layer branches each producing the SED as multi-class multilabel classification and DOA as multi-output regression; together producing the SELD output.

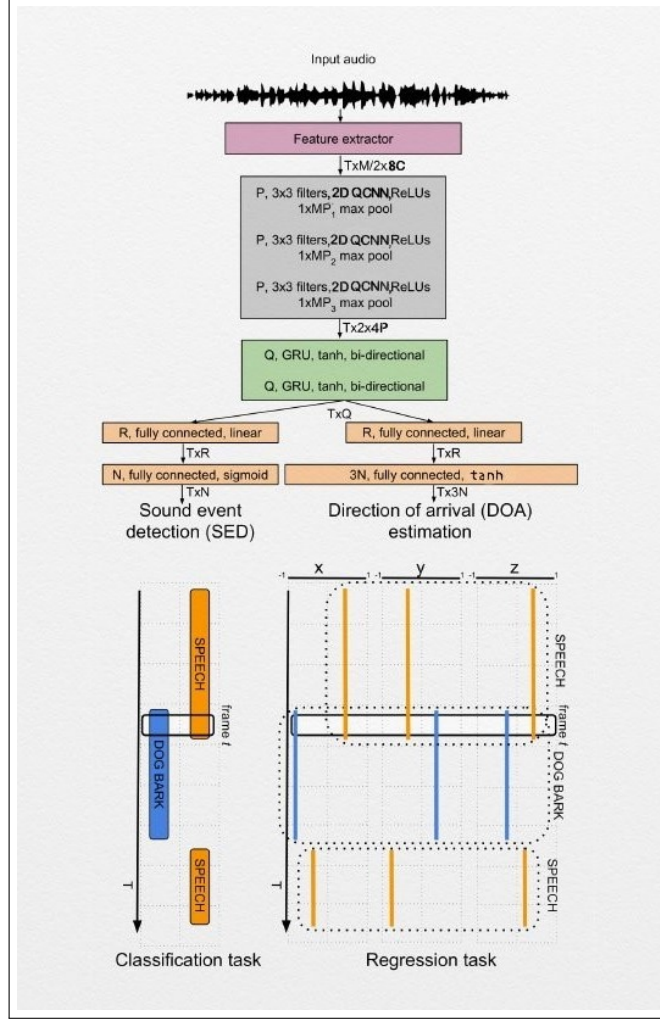


Figure 1: Quaternion Convolutional Neural Network

### 3.1 Weight Initialization

The appropriate and correct initialization of the network parameters in the quaternion domain must take into account the interactions between quaternion-valued components, thus a simple random and component-wise initialization may result in an unsuitable choice.

A possible solution maybe derived by considering a normalized purely quaternion  $u^{\triangleleft}$  generated for each weight  $w$  by following a uniform distribution in  $[0, 1]$ .

Each weight can be written in a polar form as:

$$w = |w|e^{u^{\triangleleft}\theta} = |w|(\cos \theta + u^{\triangleleft} \sin \theta)$$

from which it is possible to derive the quaternion-valued components of  $w$ :

$$\begin{cases} w_W = \phi \cos(\theta) \\ w_X = \phi u_X^{\triangleleft} \sin(\theta) \\ w_Y = \phi u_Y^{\triangleleft} \sin(\theta) \\ w_Z = \phi u_Z^{\triangleleft} \sin(\theta) \end{cases}$$

where  $\theta$  is randomly generated in the range  $[-\pi, \pi]$  and  $\phi$  is a randomly generated variable related to the variance of the quaternion weight, defined as  $\text{var}(W) = E\{|W|\} - (E\{|W|\})^2$ . where the second term is null

due to the symmetric distribution of the weight around 0. Since  $W$  follows a Chi distribution with four degrees of freedom, the variance can be expressed as:

$$var(W) = E\{|W|^2\} = \int_0^\infty w^2 f(w) dw = 4\sigma^2$$

being  $\sigma$  the standard deviation. The variable  $\phi$  can be randomly generated in the range  $[-\sigma, \sigma]$ .

## 4 Dataset

We evaluate the proposed method involving the QCRNN on a dataset, TAU Spatial Sound Events 2019 - Ambisonic, providing four-channel First-Order Ambisonic (FOA) recordings.

The recordings on the dataset consist of stationary point sources from multiple sound classes each associated with a temporal onset and offset time, and DOA coordinate represented using azimuth and elevation angle.

The dataset consists of a development and evaluation set. The development set consists of 400, one minute long recordings sampled at 48000 Hz, divided into four cross-validation splits of 100 recordings each. The evaluation set consists of 100 one-minute long recordings.

These recordings were synthesized using spatial room impulse response (IRs) collected from five indoor locations, at 504 unique combinations of azimuth-elevation-distance.

Additionally, half the number of recordings have up to two temporally overlapping sound events, and the remaining have no overlapping.

Finally, to create a realistic sound scene recording, natural ambient noise collected in the IR recording locations was added to the synthesized recordings such that the average SNR of the sound events was 30 dB.

The only explicit difference between each of the development dataset splits and evaluation dataset is the isolated sound event examples employed.

The dataset consists of eleven sound event classes, each with 20 examples: knock, drawer, clearthroat, phone, keysDrop, speech, keyboard, pageturn, cough, doorslam and laughter.

The dataset contains 250 audio files, randomly divided into five splits in a way that in each split there is an equal number of examples for each class: we used the first four for training the network, while the remaining one is used for testing (20%).

We wrote a Python script in order to divide the dataset in the right way. The script automatically divides the samples and creates the directories that the program expects to receive.

The main division is about the number of overlaps, we have samples with two and one overlap. For each one of these subsets we have two directories: one with the file audio (in wav format) and the other for the labels (in csv format). The dataset results to be divided in 4 directories.

## 5 Metrics

The SELD task can use individual SED and localization (DOA) metrics.

For the SED task, we use the polyphonic SED metrics that are the F-score (ideally  $F = 1$ ), based on the number of true and false positives, and the error rate (ER) (ideally  $ER = 0$ ), based on the total number of active sound event classes in the ground truth.

A joint SED score can be considered as  $S_{SED} = \frac{(ER + (1 - F))}{2}$ .

On the other hand, in order to measure the performance of the localization task, a DOA estimation error  $DOA_{err}$  can be used as evaluation metric, based on estimated and ground truth DOAs.

Moreover, a frame recall metric  $K$  (ideally  $K = 1$ ) can be used based on the percentage of true positives.

A joint DOA score can be defined as  $S_{DOA} = \frac{(DOA_{err}/180 + (1 - K))}{2}$ .

The lower the  $S_{DOA}$  score, the better the results in terms of 3D localization. Finally, an overall SELD score can be defined based on the previous metrics as  $S_{SELD} = \frac{(S_{SED} + S_{DOA})}{2}$ .

## 6 Experimentation

We did experiments using two different approaches. After training, we computed confidence interval for each model that we created.

## First Experiment

In the first case we trained the Quaternion based neural network with two different values for the hyperparameter of the network, in particular we changed the number of filters in the Quaternion convolutional layers, in order to discover what is the behavior of the network and its results with respect to the different parameters.

We did our experiments trying the values 16 and 32 for the hyperparameter of the number of filters (the hyperparameter  $\mathbf{P}$ ) in the QCNN layers. This led to a huge difference in the number of parameters of the models. While in the model with 16 filters there are 270.657 trainable parameters in the model with 32 there are 425.985 parameters. We leave unchanged all the other parameters with these values: window length  $M=512$ , sequence length  $T=512$  of frames, batch size 10,  $Q=128$  nodes for the recurrent network and 32 nodes for fully connected layers.

We trained this two models on both the datasets (with one overlap (**ov1**) and two overlaps (**ov2**)). Of course, the models trained on the dataset with two overlaps performs worse than the models trained on the dataset with only one overlap. In fact, having two different sound sources in the same time instant makes the problem of detecting and localizing the sources a lot more complex to solve for the network.

We trained the models for  $\sim 150$  epochs.

We discovered that the network with 32 number of filters in the QCNN layers performs slightly better than the model with only 16 filters.

## Second Experiment

In our second experiment, we compared the traditional approach used in this kind of problems (the Seld network based on normal convolutional layers) with the Quaternion based neural network.

We trained both networks with the same data and studied the results.

We couldn't extract the feature in the same way for both the models because they expect different inputs. While the traditional model expects as input some Fourier transformed values, our network expects it in a Quaternion form. For this reason, we had to run two different scripts for extracting the features in the two different ways.

For training our QCRNN, we used the winning configuration of our first experiment (with 32 filters in the Quaternion Convolutional layers).

In the Seld Network we used the default parameters used by Sharath Adavanne, Archontis Politis, and Tuomas Virtanen in their work with the Seld-net.

We trained the models for  $\sim 150$  epochs.

## 7 Results

### QCRNN with 32 filters in the Quaternion Convolutional layers

The results made using the neural network set with 32 filters in the convolutional layer are shown.

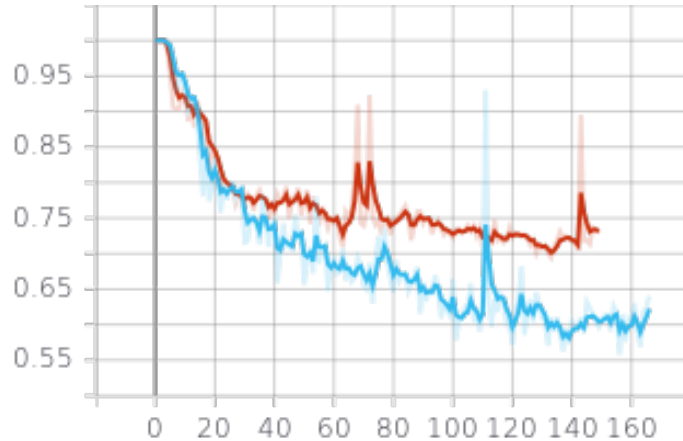


Figure 2:  $S_{SED}$  evolution computed on the test set during the training

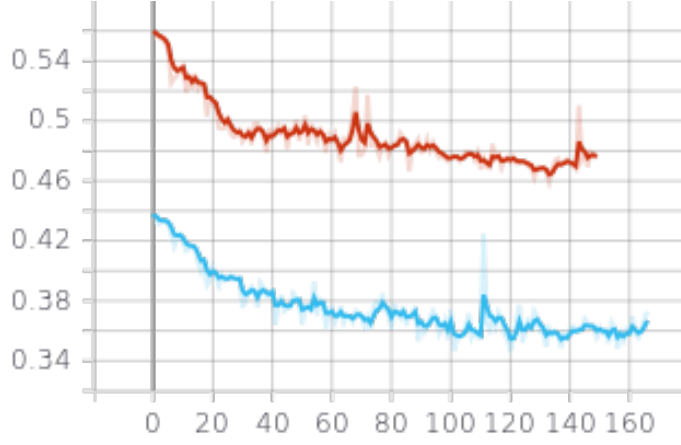


Figure 3:  $S_{DOA}$  evolution computed on the test set during the training

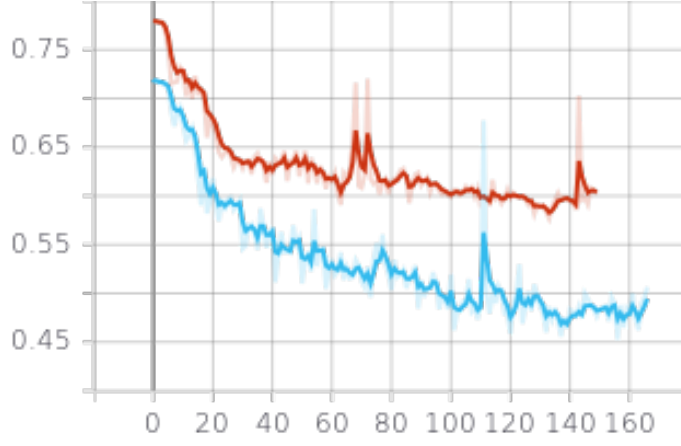


Figure 4:  $S_{SELD}$  evolution computed on the test set during the training

We can see what we have achieved with the same network on both the two overlaps (ov1 and ov2). The red line refers to the 32 filter network trained on the samples with 2 overlaps (ov2), while the light blue line refers to the same network trained on samples with a single sound overlap (ov1). Indeed, what can be seen from the graphs above is that the network performs better with samples with a single overlap than that with two overlaps. This is because the second overlap makes the sound less clear and more difficult to locate and reveal. In both cases the  $S_{SED}$  score,  $S_{DOA}$  score and  $S_{SELD}$  score drop as the epoch increases, this means that the network continuously improves the results in order to obtain more and more better performances.

		QCRNN
O1	<i>Error rate</i>	0.6122
	<i>F1 – score</i>	0.4972
	$S_{SED}$	0.5575
	$S_{DOA}$	0.3478
	$S_{SELD}$	0.4527
O2	<i>Error rate</i>	0.7529
	<i>F1 – score</i>	0.3646
	$S_{SED}$	0.6941
	$S_{DOA}$	0.459
	$S_{SELD}$	0.5766

Table 1: The best results of the network on the TAU Dataset in terms of the SED score, DOA score and SELD score considering neural network with 32 filters in the quaternion convolutional layers. In the case of ov1 we obtained the best values in epoch 156, instead for ov2 in epoch 133.

## Experiments carried out: QCRNN 16, QCRNN 32 and CNN

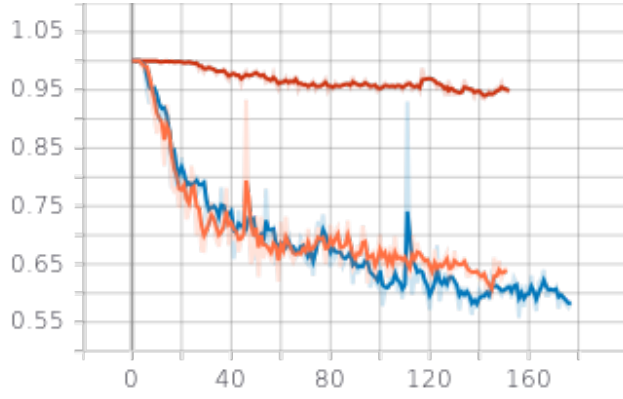


Figure 5:  $S_{SED}$  Score on ov1

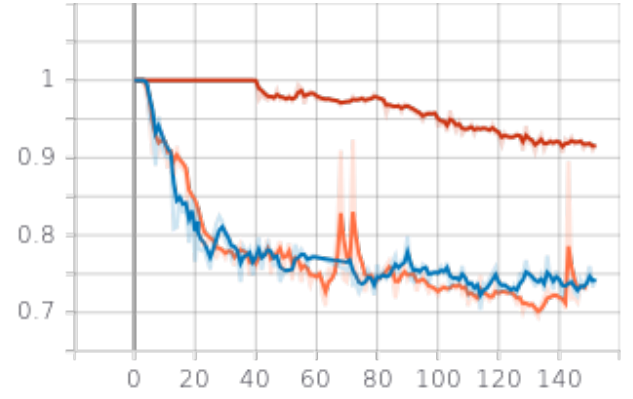


Figure 6:  $S_{SED}$  Score on ov2

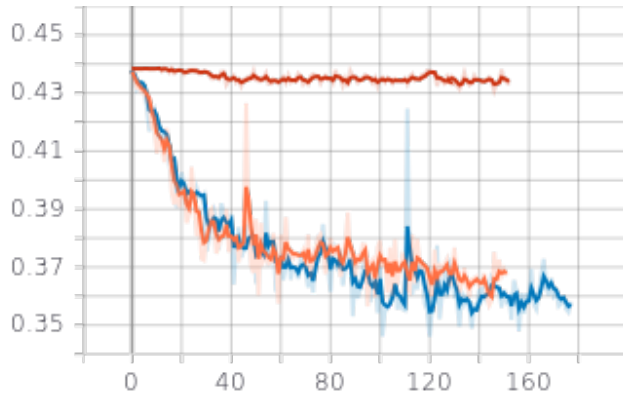


Figure 7:  $S_{DOA}$  Score on ov1

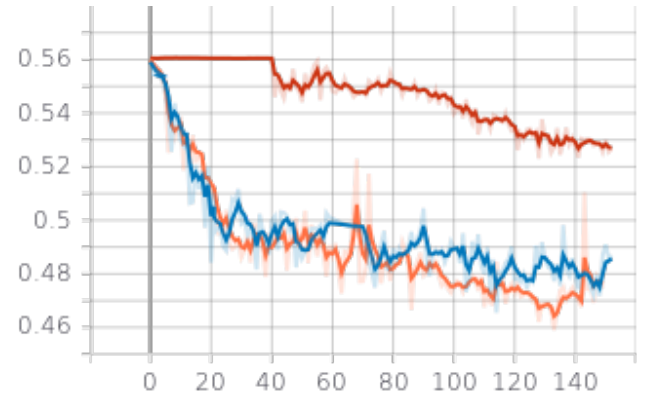


Figure 8:  $S_{DOA}$  Score on ov2

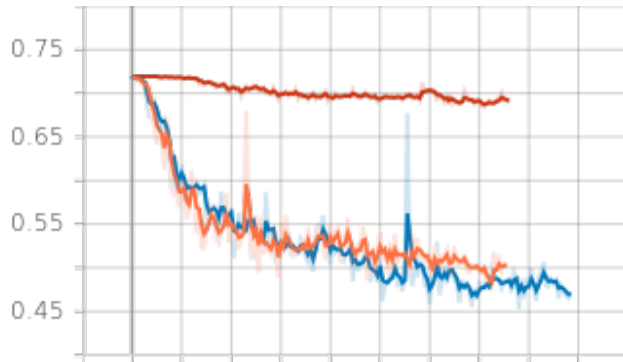


Figure 9:  $S_{SELD}$  Score on ov1

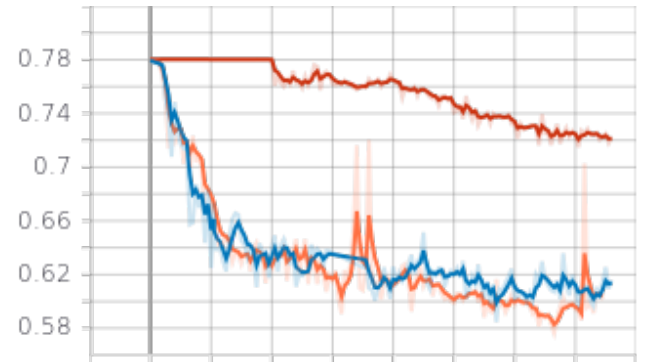


Figure 10:  $S_{SELD}$  Score on ov2

- (a) **orange**: QCRNN net with 16 filters in the quaternion convolutional layers;
- (b) **blue**: QCRNN net with 32 filters in the quaternion convolutional layers;
- (c) **red**: Traditional Seld-net CRNN approach with default parameters;

- (a) **blue**: QCRNN net with 16 filters in the quaternion convolutional layers;
- (b) **orange**: QCRNN net with 32 filters in the quaternion convolutional layers;
- (c) **red**: Traditional Seld-net CRNN approach with default parameters;



		QCRNN 16	QCRNN 32	CNN-SELDnet
O1	<i>Error rate</i>	0.6666	0.6122	0.9444
	<i>F1 – score</i>	0.4625	0.4972	0.07491
	<i>S<sub>SED</sub></i>	0.5976	<b>0.5575</b>	0.9401
	<i>S<sub>DOA</sub></i>	0.3586	<b>0.3478</b>	0.434
	<i>S<sub>SELD</sub></i>	0.4781	<b>0.4527</b>	0.6843
O2	<i>Error rate</i>	0.7607	0.7529	0.9323
	<i>F1 – score</i>	0.3538	0.3646	0.1126
	<i>S<sub>SED</sub></i>	0.7035	<b>0.6941</b>	0.9147
	<i>S<sub>DOA</sub></i>	0.4655	<b>0.459</b>	0.5268
	<i>S<sub>SELD</sub></i>	0.5845	<b>0.5766</b>	0.7208

Table 2: The best results on the TAU Dataset in terms of the SED score, DOA score and SELD score considering several experiments. We considered the values referred to the best epoch for each model.

## 8 Conclusion

Confronto tra i risultati ottenuti dall’esperimenti di 32. In particolare le differenze tra i due overlap (ov1 e ov2). Confronto tra i risultati di 16 con quelli da 32, in particolare tra i due overlap (cioè i ov1 separati da ov2). Inoltre, evidenziare che con 32 si ottengono risultati migliori. Spiegazione del perchè 32 è meglio. Analisi complessiva delle diffeze dell’andamento della rete dei quaternioni con quella normale (CNN). In particolare, sottolineando che quella dei quaternioni risulta essere migliore e perchè.